

# Analytical Two-Phase Flow Void Prediction Method

Reazul Huq\*

*BWR Thermal Hydraulics, SIEMENS/KWU, Offenbach, Germany*

and

John L. Loth†

*West Virginia University, Morgantown, West Virginia 26506*

An analytical formula has been derived, without empirical constants, that predicts the lower limit void fraction as a function of quality and pressure. The derivation utilizes a functional relationship for the slip and the boundary conditions at the limits as  $\chi \rightarrow 0$  and  $\chi \rightarrow 1$ . The formula has been compared with two state-of-the-art correlations, in the parameter range of operation of a Boiling Water Reactor (BWR) at steady state, and with some air–water data. It fits the first case data rather well, and correlates the air–water data with even greater accuracy. The potential applicability of this formula to countercurrent flow cases has not yet been explored. This paper concentrates on the derivation of the formula and comments on the data correlations.

## Nomenclature

$A$	= flow area, m <sup>2</sup> (without subscript: total flow area)
$C_0$	= parameter defined in text
$F$	= intermediate function defined in text
$f$	= intermediate function defined in text
$g$	= intermediate function defined in text
$\dot{m}$	= mass flow rate, kg/s (without subscript: total flow rate)
$S$	= slip, velocity ratio $V_g/V_l$
$V$	= average velocity of each phase
$V_{gj}$	= parameter defined in text
$\alpha$	= void fraction, area ratio $A_g/A$
$\rho$	= fluid phase density, kg/m <sup>3</sup>
$\chi$	= flow quality, mass flow ratio $\dot{m}_g/\dot{m}$

## Subscripts

$g$	= gas phase
$l$	= liquid phase

## Introduction

AMONG the best known correlations for void fraction prediction in two-phase flow are the works of EPRI,<sup>1</sup> GE,<sup>2</sup> Ohkawa et al.,<sup>3</sup> Holmes,<sup>4</sup> and Ishii.<sup>5</sup> The general basis for these correlations is predominantly due to Zuber and Findlay's<sup>6</sup> void drift model:  $\alpha = \alpha(\chi, C_0, V_{gj})$ . The concentration parameter  $C_0$  and the drift velocity parameter  $V_{gj}$  are independent of one another but both are functions of the void fraction  $\alpha$ .

The appropriate formulations required to arrive at such an implicit expression for data correlation are necessarily complex but have the advantage that they incorporate a "mass flux effect" not described by the previous works. The effect that heat flux and liquid-to-vapor viscosity ratio has on the void fraction is known from experiments, see Ref. 7, but is not accounted for in this analysis. Surface roughness is yet another factor not considered. The quantitative evaluation of the individual effects is difficult. The void fraction data gen-

erally encompass all such effects. Thus fits of data using correlations that contain only mass flux effects may overestimate the influence of the mass flux. Studies indicate that a possible approach to combine such composite effects is through the use of the variable entropy. The entropy production rate quantifies the irreversibility in the convective heat transfer process in a duct and encompasses the cumulative effect of all parameters. It enhances the local flow quality in the duct and hence the corresponding void fraction. A reduced irreversibility is accompanied by a less pronounced "mass flux effect."

In this context the Imperial College data,<sup>8</sup> with adiabatic air–water mixture, will be examined later. The data appear to result in a single void-quality curve that contains a 25-fold mass flux variation. The expected "mass flux effect" was absent. In this case the entropy production rate is relatively low. One may anticipate that for zero entropy production rate (reversible case) there may exist an "ideal" void-quality relationship with slippage but devoid of other irreversibilities. This should approach the air–water data. Since any additional process irreversibility must increase the void fraction, the "ideal curve" should represent the lower limit of void curves at any given pressure. The subject of this paper is the development of a formula that provides the lower limit void curve, without resorting to empirical constants. A comparison of the resulting formula with some data and state-of-the-art correlations is discussed. Butterworth,<sup>9</sup> compared six apparently dissimilar void fraction correlations, some of which included the liquid/vapor viscosity ratio, and found all of them to be very similar! This explains why the correlation presented here, which is only a function of pressure, has the potential for comparing well with others that include all effects.

## Analysis

Consider the flow of a two-phase gas–liquid mixture in a tube. The gas mass flow fraction at any cross section is expressed in terms of the flow quality  $\chi$ . This is defined as

$$\chi = \frac{\dot{m}_g}{\dot{m}} = \frac{\dot{m}_g}{\dot{m}_g + \dot{m}_l} \quad (1)$$

Thus  $\chi$  can only assume values between 0 and 1. The fraction of the tube cross-sectional area  $A$  occupied by the gas phase at any location is called the void fraction  $\alpha$  defined as

$$\alpha = \frac{A_g}{A} = \frac{A_g}{A_g + A_l} \quad (2)$$

Received May 4, 1990; presented as Paper 90-1738 at the AIAA/ASME 5th Joint Thermophysics and Heat Transfer Conference, Seattle, WA, June 18–20, 1990; revision received Dec. 7, 1990; accepted for publication Dec. 7, 1990. Copyright © 1991 by the American Institute of Aeronautics and Astronautics, Inc. All rights reserved.

\*Reactor Division.

†Professor, Department of Mechanical and Aerospace Engineering. Associate Fellow AIAA.

Accordingly,  $\alpha$  can only assume values between 0 and 1. The objective is to find  $\alpha$  as a function of  $\chi$ . The effect that heat transfer has on the quality  $\chi$  is not discussed in this paper. In the following derivations, cross-sectional average values have been used for those parameters that vary with radius over the cross section of the tube. Equations (1) and (2) can be coupled and the result written in terms of the ratio: average liquid-to-vapor density and the ratio of average velocities of the phases

$$\frac{1}{\chi} = 1 + \frac{\dot{m}_l}{\dot{m}_g} = 1 + \frac{\rho_l}{\rho_g} \cdot \frac{V_l}{V_g} \cdot \frac{A_l}{A_g} \quad (3)$$

Denote the velocity ratio  $V_g/V_l$  by the slip into  $S$ , and express the area ratio  $A_l/A_g$  in terms of the void fraction  $\alpha$ . The result is

$$\frac{1}{\chi} - 1 = (\rho_l/\rho_g) \cdot \frac{1}{S} \left( \frac{1}{\alpha} - 1 \right) \quad (4)$$

Solve Eq. (4) for  $\alpha$  to obtain the classical void formula:

$$\alpha = \frac{\chi}{\chi + (1 - \chi) \cdot (\rho_g/\rho_l) \cdot S} \quad (5)$$

All quantities on the right-hand side are known or given except for the average slip  $S$ , the determination of which is part of this derivation. For shorter notation a variable  $g(\chi)$  is introduced

$$g(\chi) = \frac{\rho_g}{\rho_l} \cdot S \leq S \quad (6)$$

In most practical applications the density ratio in Eq. (6) is less than 1. It is equal to 1 only at the critical pressure (= 221.1 bar for water). The classical void formula (5) reduces to

$$\alpha = \frac{\chi}{\chi + (1 - \chi) \cdot g(\chi)} \quad (7)$$

Most state-of-the-art void fraction correlations are fits to extensive ( $\chi$ ,  $\alpha$ ) data bases. In such correlations, slip does not appear explicitly. However, utilizing the classical void formula (5) one can calculate the corresponding slip value.

Observe in Eq. (7) that the magnitude of  $[\rho_l/\rho_g]/S$  determines whether  $\alpha$  is greater or smaller than  $\chi$ . For normal reactor operational pressure  $(\rho_l/\rho_g) \geq 1$  and  $(\rho_l/\rho_g)/S > 1$ , buoyancy in a vertical tube tends to increase  $S > 1$  but not enough to offset the density ratio. At a typical BWR pressure of 70 bar, steam tables provide a value of 20.7 for the density ratio. Therefore from Eq. (4) follows that in general  $(1/\chi) \geq (1/\alpha)$  or the flow quality  $\chi$  is less than the void fraction  $\alpha$ . At the critical pressure both phases have the same density and there is no buoyancy force to drive slip. In that case both  $S$  and  $g(\chi)$  reduce to 1, thus at critical pressure  $\chi = \alpha$ , shown as a 45-deg line on a linear  $\chi$ - $\alpha$  graph.

Most state-of-the-art void correlations contain a mass flux dependency of the void fraction. With decreasing mass flux such correlations may result in  $\chi > \alpha$  which conflicts with the above made conclusion that  $\chi \leq \alpha$  in between the endpoints. Although the functional relationship between  $\alpha$  and  $S$  is not known, their characteristic behavior near the endpoint 0 and 1 can be determined.

### Endpoint Conditions on S

Consider an *ideal* friction-free liquid flowing with *uniform velocity* inside a tube with heated walls. Starting at  $\chi = 0$ , as the first vapor bubbles separate from the walls, the liquid serves as the carrier medium, forcing the initial bubble ve-

locity to equal that of the surrounding liquid. In this case the gas/liquid velocity ratio  $S$  approaches 1. At the other extreme when  $\chi \rightarrow 1$  and most of the mass flow has evaporated to steam, the vapor becomes the carrier for the few remaining small liquid droplets and the slip  $S$  approaches 1.

In a *real* fluid, flowing in a tube, the velocity is reduced near the wall. Thus when the first bubbles separate from the wall, their initial bubble velocity will be well below the bulk average velocity inside the tube. In that case,  $S < 1$  for  $\chi \rightarrow 0$ . Summarizing the above

$$\text{for } \chi \rightarrow 0: \quad \alpha \rightarrow 0, S < 1$$

$$\text{for } \chi \rightarrow 1: \quad \alpha \rightarrow 1, S \rightarrow 1 \quad (8)$$

Alia et al.<sup>10</sup> published observations that tend to confirm the second endpoint condition on slip in Eq. (8), although the actual measurements could not be carried out at these extreme void conditions.

### Endpoint Conditions on $\alpha$

Prior to the onset of boiling, both  $\chi$  and  $\alpha$  are 0. When the process of evaporation is completed,  $\chi$  becomes 1 and the corresponding void fraction also becomes 1. Accordingly, when plotting  $\alpha$  versus  $\chi$  on a linear plot, all curves must pass through the points  $(\chi, \alpha) = (0, 0)$  and  $(1, 1)$ .

The slopes of the  $\alpha$  versus ( $\chi$ ) curve, at the endpoint conditions, are found from Eq. (7) using the first derivative

$$\begin{aligned} \frac{d\alpha}{d\chi} &= \frac{1}{\chi + (1 - \chi)g(\chi)} \\ &\quad - \frac{\chi \left( 1 + \frac{dg(\chi)}{d\chi} - g(\chi) - \chi \frac{dg(\chi)}{d\chi} \right)}{[\chi + (1 - \chi)g(\chi)]^2} \\ &= \frac{g(\chi) + \frac{dg(\chi)}{d\chi} (\chi - \chi^2)}{[\chi + (1 - \chi)g(\chi)]^2} \end{aligned} \quad (9)$$

Taking the limits of Eq. (9) at the endpoints

$$\left. \frac{d\alpha}{d\chi} \right|_{\chi \rightarrow 0} = \lim_{\chi \rightarrow 0} \frac{1}{g(\chi)} = \frac{\rho_l}{\rho_g} \lim_{\chi \rightarrow 0} \frac{1}{S} \quad (10)$$

$$\left. \frac{d\alpha}{d\chi} \right|_{\chi \rightarrow 1} = \lim_{\chi \rightarrow 1} g(\chi) = \frac{\rho_g}{\rho_l} \lim_{\chi \rightarrow 1} S \quad (11)$$

Utilizing the result from Eq. 8 as  $\chi \rightarrow 0$  then  $S < 1$ :

$$\left. \frac{d\alpha}{d\chi} \right|_{\chi \rightarrow 0} \geq \frac{\rho_l}{\rho_g} \quad (12a)$$

At 70 bar, for flow in thermal equilibrium, the density ratio for water is 20.7. The corresponding minimum value of the slope according to Eq. (12a) is then  $\arctan 20.7 = 87^\circ$ , shown in Fig. 1. At the other limit when  $\chi$  approaches 1 and the last liquid droplets are evaporating find  $S$  approaching 1. This would produce a slope for  $\alpha(\chi)$  equal to the equilibrium density ratio. Prior to reaching this condition the thermodynamic nonequilibrium produces local superheat, which makes the average vapor density less than that of the saturated vapor. Thus from Eq. (11)

$$\left. \frac{d\alpha}{d\chi} \right|_{\chi \rightarrow 1} \leq \frac{\rho_g}{\rho_l} \quad (12b)$$

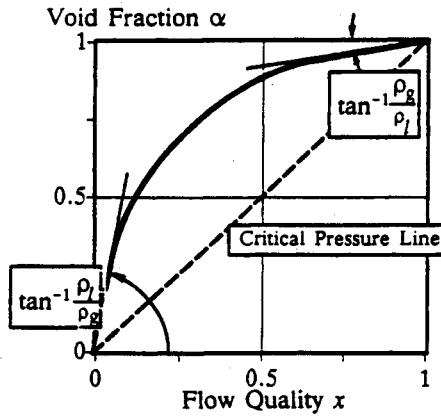


Fig. 1 Void curve schematic showing endpoint slopes and the critical pressure line.

Consequently, the slope of the curve at  $\chi = 1$  with a pressure of 70 bar must be less than  $\arctan(1/20.7) = 3$  deg, as shown in Fig. 1. In this case at the low end with  $\chi = 1\%$  expect  $\alpha \approx 20.7\%$ , the associated reduction in liquid flow passage area may significantly increase the local liquid velocity and reduce pressure. Because the void fraction is most important in the low-quality range, it is better to show the  $\alpha$ - $\chi$  relationship on a semilog plot. Most plots use a linear scale for  $\alpha$  from 0 to 1, and a logarithmic scale for  $\chi$  from 0.001 to 1. In summary the endpoint slopes are

$$\begin{aligned} \text{for } \chi \rightarrow 0: \quad \alpha \rightarrow 0, \quad \left. \frac{d\alpha}{d\chi} \right|_{\chi=0} &\geq \frac{\rho_l}{\rho_g} \\ \text{for } \chi \rightarrow 1: \quad \alpha \rightarrow 1, \quad \left. \frac{d\alpha}{d\chi} \right|_{\chi=1} &\leq \frac{\rho_g}{\rho_l} \end{aligned} \quad (13)$$

The equal signs in the expressions for the slope refer to the ideal fluid case with uniform velocity over the cross section and thermal equilibrium.

#### Introducing a New Function $F(\chi)$

Having defined the required characteristics of the  $\alpha(\chi)$  curve at the endpoints, the objective is to derive an  $\alpha$ - $\chi$  relationship that satisfies the endpoint conditions and is in agreement with the data. Consider first the slip ratio  $S$  in Eq. (5). Solving for  $S$  one obtains

$$\begin{aligned} \frac{1}{S} &= \frac{(1-\chi)(\rho_g/\rho_l)}{\chi \cdot (1/\alpha - 1)} = \frac{(1-\chi) \cdot \frac{\alpha}{1-\alpha}}{\chi(\rho_l/\rho_g)} \\ &= \frac{(1-\chi) \cdot \frac{1 - A_l/A}{A_l/A}}{\chi \cdot (\rho_l/\rho_g)} = \frac{1-\chi}{\chi \cdot (\rho_l/\rho_g)} - (1-\chi) \end{aligned} \quad (14)$$

In the second to last step, Eq. (2) has been used to replace  $\alpha$  by the area ratio. The area ratio term can be modified using Eqs. (1) and (3) by writing the liquid mass flow rate as

$$\dot{m}_l = \rho_l V_l A_l = \dot{m} \cdot (1 - \chi) \quad (15)$$

Divide Eq. (15) by the flow area  $A$  and rearrange

$$\frac{(1-\chi)}{A_l/A} = \frac{\rho_l V_l}{\dot{m}/A} \quad (16)$$

Insert Eq. (16) into Eq. (14) to obtain a modified expression for the slip:

$$\frac{1}{S} = \frac{V_l}{V_g} = \frac{\frac{\rho_l \cdot V_l}{\dot{m}/A} - (1-\chi)}{\chi \cdot (\rho_l/\rho_g)} \quad (17)$$

Equation (17) can be conveniently used to investigate the behavior of the liquid velocity as a function of  $\chi$ . From continuity one knows that for  $\chi \rightarrow 0$ ,  $(\rho_l V_l)/(\dot{m}/A) \rightarrow 1$ . Inserting this in Eq. (17) leads to  $1/S \rightarrow 0/0$ . As established previously, when  $\chi$  approaches 0 the slip  $S$  is finite, applying L'Hospital rule on Eq. (17) gives:

$$\lim_{\chi \rightarrow 0} \frac{V_l}{V_g} = \frac{\frac{A}{\dot{m}} \cdot \frac{dV_l}{d\chi} \Big|_{\chi \rightarrow 0} + \frac{1}{\rho_l}}{\frac{1}{\rho_g}} \rightarrow 1 \quad (18)$$

The RHS of Eq. (18) can be rearranged using its limiting value of 1 indicated above to get

$$\left. \frac{dV_l}{d\chi} \right|_{\chi \rightarrow 0} = \left( \frac{1}{\rho_g} - \frac{1}{\rho_l} \right) \cdot \frac{\dot{m}}{A} \quad (19)$$

Equation (19) provides the value of the slope of the liquid velocity at the lower limit of  $\chi$ . As bubbles are formed, the passage area  $A_l$  for the remaining liquid is reduced. In order to satisfy continuity, the average liquid velocity must increase with increasing void fraction and associated flow quality  $\chi$ . This yet unknown functional relationship between the variation of the liquid velocity with increasing  $\chi$  is formally obtained by introducing an arbitrary function  $f(\chi)$  as shown below:

$$\frac{dV_l}{d\chi} = \left( \frac{1}{\rho_g} - \frac{1}{\rho_l} \right) \frac{\dot{m}}{A} \cdot f(\chi) \quad (20)$$

Integrate Eq. (20) in the range from 0 to  $\chi$ , which results in:

$$\begin{aligned} \int_{V_l(0)}^{V_l(\chi)} dV_l &= \int_0^\chi \left( \frac{1}{\rho_g} - \frac{1}{\rho_l} \right) \cdot \frac{\dot{m}}{A} \cdot f(\chi) d\chi \\ \times V_l(\chi) &= \left( \frac{1}{\rho_g} - \frac{1}{\rho_l} \right) \cdot \frac{\dot{m}}{A} \cdot F(\chi) + \frac{\dot{m}}{A\rho_l} + C \end{aligned} \quad (21)$$

where  $F(\chi) = \int_0^\chi f(\chi) d\chi$

In order to satisfy Eq. (19), in the limit as  $\chi \rightarrow 0$ , the function  $f(\chi)$  must equal 1, or

$$\left. \frac{dF(\chi)}{d\chi} \right|_{\chi=0} = f(\chi) \Big|_{\chi=0} = 1 \quad (22)$$

In the above, the unknown function  $f(\chi)$  defines another function  $F(\chi)$  whose properties are more easily determined than those of  $f(\chi)$ .

At  $\chi = 0$ , insert the definition of  $V_l$  from Eq. (15) into Eq. (21). The constant of integration  $C$  can then be eliminated as long  $F(\chi) = 0$ .

$$F(\chi) \Big|_{\chi=0} = 0 \quad (23)$$

At  $\chi = 1$  the slip must approach the value 1. Consequently, the following relation holds

$$V_l \Big|_{\chi=1} = V_g \Big|_{\chi=1} = \frac{\dot{m}}{A\rho_g} \quad (24)$$

Inserting Eq. (24) into Eq. (21) for the limiting case of  $\chi = 1$  and recalling that  $C = 0$ , one obtains the following additional condition on  $F(\chi)$ :

$$F(\chi) \Big|_{\chi=1} = 1 \quad (25)$$

If one inserts Eq. (21) into Eq. (17) an expression for  $S$  in terms of  $F(\chi)$  results:

$$\frac{1}{S} = \frac{V_\ell}{V_g} = \frac{\left(\frac{1}{\rho_g} - \frac{1}{\rho_\ell}\right) \cdot F(\chi) + \frac{\chi}{\rho_\ell}}{\chi/\rho_g} \quad (26)$$

Recall that in the classical void formula [Eq. (5)] the only unknown was  $S$ . Equation (26) would provide  $S$  if  $F(\chi)$  could be determined. Note only two conditions on  $S$ , at both  $\chi = 0$  and  $\chi = 1$  are known, but the above analysis provides three conditions on  $F(\chi)$ , as given by Eqs. (22), (23), and (25). Another property of  $F(\chi)$  can be extracted from Eq. (26). For example, at critical pressure the slip  $S$  is unity over the whole range of  $\chi$ , which then reduces Eq. (26) to  $\chi = F(\chi)$ . Thus the behavior of  $F(\chi)$  and  $\alpha$  is similar at critical pressure. At very low pressure one can ignore the density ratio relative to 1, and Eq. (26) can be reduced to

$$\frac{1}{S} = \frac{(1 - \rho_g/\rho_\ell) \cdot F(\chi) + \chi \cdot (\rho_g/\rho_\ell)}{\chi} \cong \frac{F(\chi)}{\chi} \quad (27)$$

### Determination of $F(\chi)$

The conditions to be fulfilled by  $F(\chi)$  according to Eqs. (22), (23), and (25) are repeated below for convenience:

$$F(\chi)|_{\chi=0} = 0; \quad F(\chi)|_{\chi=1} = 1; \quad \frac{dF(\chi)}{d\chi} \Big|_{\chi=0} = 1 \quad (28)$$

Numerous functions could be proposed for  $F(\chi)$  which satisfy Eq. (28). However, one may observe that the inclusion of a constant, such as the fluid density, would not alter the preceding development of the function  $F(\chi)$ . Such a property dependency cannot be arbitrary because one must ensure that the resulting expressions for  $S$  and  $\alpha$  do not violate their previously established endpoint conditions and other characteristics. In an attempt to establish an appropriate function for  $F(\chi)$ , one may observe that the preceding discussion has shown points of close resemblance between the functions  $F(\chi)$  and  $\alpha(\chi)$ :

- 1) Both are dependent on  $\chi$  and fluid property.
- 2) They behave identically at critical pressure.
- 3) Both satisfy identical endpoint conditions.

Nonresemblance between the functions consists only in their slopes at  $\chi = 0$ . At this limiting point the slope of  $\alpha(\chi)$ , as determined by the function  $g(\chi)$  in Eq. (7), is given by Eq. (10) in the form

$$\lim_{\chi \rightarrow 0} \frac{1}{g(\chi)} = \frac{\rho_\ell}{\rho_g}$$

At  $\chi \rightarrow 0$ ,  $g(\chi)$  acts as the slope determining function of  $\alpha(\chi)$ . The slope of  $F(\chi)$ , on the other hand, is unity irrespective of the fluid properties, as shown in Eq. (28); at all other values of  $\chi$  it may be property dependent. Consequently, an appropriate functional form for  $F(\chi)$  could be similar to that of  $\alpha(\chi)$ , but with a different slope determining function  $\omega(\chi) \neq g(\chi)$ . Hence the following format is proposed here:

$$F(\chi) = \frac{\chi}{\chi + (1 - \chi)\omega(\chi)} \quad (29a)$$

Obviously, at  $\chi = 0$  the restriction

$$\omega(\chi)|_{\chi=0} = 1$$

applies. In order to find  $\omega(\chi)$ , note that for the case of  $\chi = 0$  one can rearrange Eq. (21), the basic expression for the liquid phase velocity  $V_\ell(\chi)$ , which contains  $F(\chi)$ , to obtain

$$\frac{\rho_\ell V_\ell(\chi)}{\dot{m}/A} \Big|_{\chi=0} = 1$$

This leads to the observation that the two terms

$$\omega(\chi) \Big|_{\chi=0} = 1 \text{ corresponds to } \frac{\rho_\ell V_\ell(\chi)}{\dot{m}/A} \Big|_{\chi=0} = 1$$

It is not known a priori whether this correspondence is extendable over all  $\chi$ . However, primarily because the above term fulfills the requirement on  $\omega(\chi)$  at  $\chi = 0$ , this term is proposed for  $\omega(\chi)$  in Eq. (29). Inserted in Eq. (29a) gives

$$F(\chi) = \frac{\chi}{\chi + (1 - \chi) \cdot \frac{\rho_\ell V_\ell(\chi)}{\dot{m}/A}} \quad (29b)$$

Observe that since the liquid velocity in Eq. (29b) already contains  $F(\chi)$  according to Eq. (21), it is an implicit formulation of  $F(\chi)$ . Combining these two equations results in a quadratic equation from which two solutions are found for  $F(\chi)$ . One of these applies to coflow and the other to counter-current flow situations.

### Verification of $F(\chi)$ and Solutions for $S$ and $\alpha$

One can easily verify that the first two conditions in Eq. (28) are fulfilled by  $F(\chi)$  in Eq. (29b). In order to check the third condition take the derivative

$$\frac{dF(\chi)}{d\chi} = \frac{\frac{\rho_\ell V_\ell}{\dot{m}/A} - \frac{\rho_\ell}{\dot{m}/A} \cdot \frac{dV_\ell}{d\chi} (\chi^2 - \chi)}{\left(\chi + (1 - \chi) \cdot \frac{\rho_\ell V_\ell}{\dot{m}/A}\right)^2}$$

or

$$\frac{dF(\chi)}{d\chi} \Big|_{\chi=0} = \frac{1}{\frac{\rho_\ell V_\ell}{\dot{m}/A}} = 1$$

This confirms that Eq. (29b) satisfies the conditions in Eq. (28). Combining Eq. (29b) and (21) gives the desired solution for  $F(\chi)$ :

$$F(\chi) = \frac{\chi}{\chi + (1 - \chi) \frac{\rho_\ell}{\dot{m}/A} \left( \left\{ \frac{1}{\rho_g} - \frac{1}{\rho_\ell} \right\} \frac{\dot{m} F(\chi)}{A} + \frac{\dot{m}}{A \rho_\ell} \right)}$$

$$F(\chi) = \frac{\chi}{\chi + (1 - \chi) \left( \left\{ \frac{\rho_\ell}{\rho_g} - 1 \right\} \cdot F(\chi) + 1 \right)}$$

$$0 = (1 - \chi) \left( \frac{\rho_\ell}{\rho_g} - 1 \right) \cdot F(\chi)^2 + F(\chi) - \chi$$

$$F(\chi) = \frac{-1 \pm \sqrt{1 + 4\chi(1 - \chi)(\rho_\ell/\rho_g - 1)}}{2(1 - \chi)(\rho_\ell/\rho_g - 1)} \quad (30)$$

The negative sign corresponds to a negative  $F(\chi)$ , which by Eq. (29b) requires the liquid velocity to be negative, whereas the vapor velocity is still positive. This corresponds to a coun-

tercurrent flow situation which occurs, for example, in accident simulation tests. The interest in analyzing such cases is a future objective. Here only the coflow case is considered and therefore the negative sign has been deleted.

Inserting Eq. (30) into Eq. (26) produces the desired expression for slip

$$S = \frac{V_g}{V_l} = \frac{\rho_l}{\rho_g} \cdot \frac{B}{B + D - 1} \tag{31}$$

where  $B = 2\chi(1 - \chi)$  and  $D = \sqrt{1 + 2B \left( \frac{\rho_l}{\rho_g} - 1 \right)}$

Substituting Eq. (31) in the classical void formula Eq. (4) gives

$$\alpha = 1 - \frac{2(1 - \chi)^2}{1 - 2\chi + D} \tag{32}$$

Equations (31) and (32) represent the desired functional relationship that obeys the physics of the flow at both limits when  $\chi$  approaches 0 and 1. The justification for the proposed format of  $F(\chi)$  in Eq. (29b) lies in the fact that it provides an  $\alpha$ - $\chi$  behavior similar to that of the state-of-the-art data fits in the standard reactor application area and reproduces the air-water data with greater accuracy than the existing correlations. In addition, the resulting formula is well behaved in the limits  $\chi \rightarrow 1$  or 0 and it eliminates nonphysical slip and void behavior, which can be encountered with other correlations.

### Comparison of $\alpha$ - $\chi$ Formula with Data

The correlations by EPRI<sup>1</sup> and GE<sup>2</sup> are widely accepted as representatives of the state of the art. The EPRI correlation probably covers the widest data base of all. Considering that

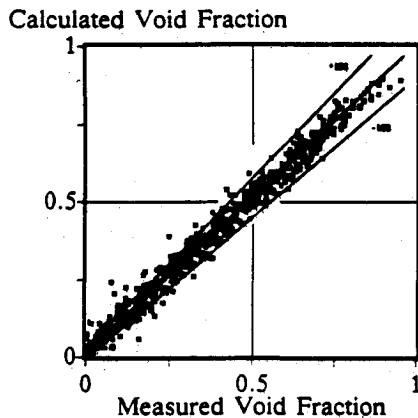


Fig. 2 Scatter of the EPRI correlation taken from Ref. 1.

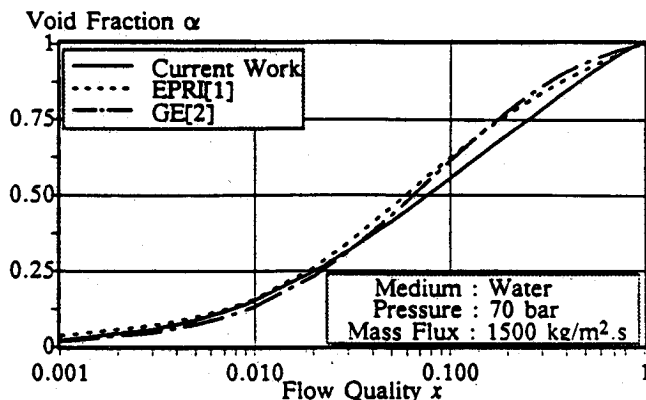


Fig. 3 Current work compared with correlations at high mass flux.

the generation of void fraction data involves complex experimental procedures, the frequently observed scatter in the acquired data need not disqualify a data base. Because of the scatter, however, a best fit through a wide variety of data bases can be taken to be more representative of the data trend than measurements of individual experimenters. Therefore, instead of comparing the current formula with individual data sets from the many workers in this field, the above two correlations are used as references. Only the air-water data are shown separately because the correlations do not appear to reproduce such data well. If one considers the scatter of the EPRI correlation in Fig. 2 taken from Ref. 1, the comparisons in Figs. 3 and 4 indicate similar behaviors of the three methods. The two mass fluxes shown roughly encompass the parameter range of operation of a BWR fuel bundle. The current formula has no mass flux dependency. Therefore, since with increasing mass flux and flow quality the entropy production rate increases, one would expect the data to show somewhat

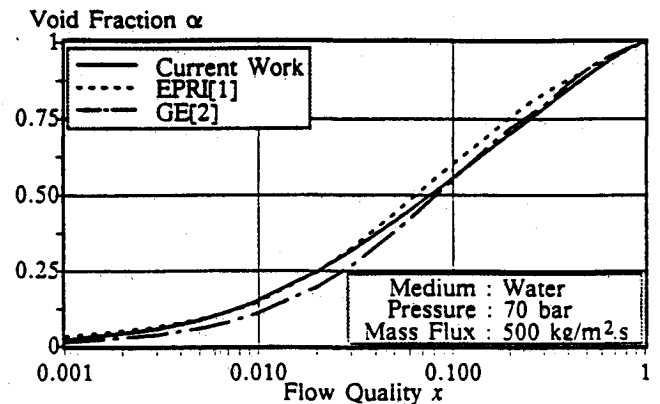


Fig. 4 Current work compared with correlations at low mass flux.

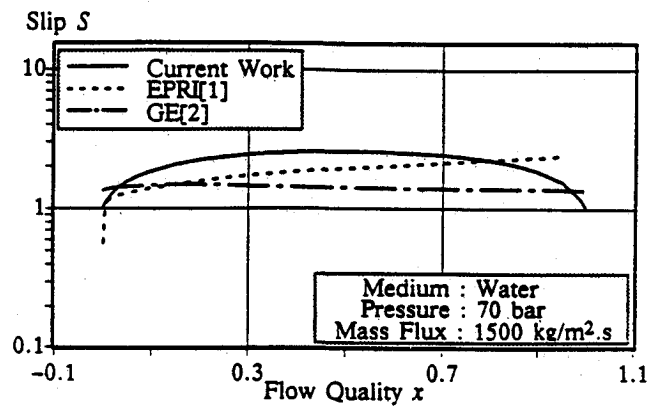


Fig. 5 Slip corresponding to void curves of Fig. 3  $x$  axis (0 to 1) artificially extended at both ends only for clarity of presentation.

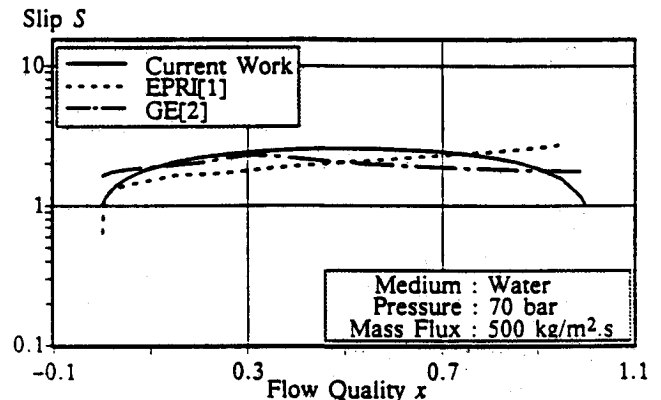


Fig. 6 Slip corresponding to void curves of Fig. 4  $x$  axis (0 to 1) artificially extended at both ends only for clarity of presentation.

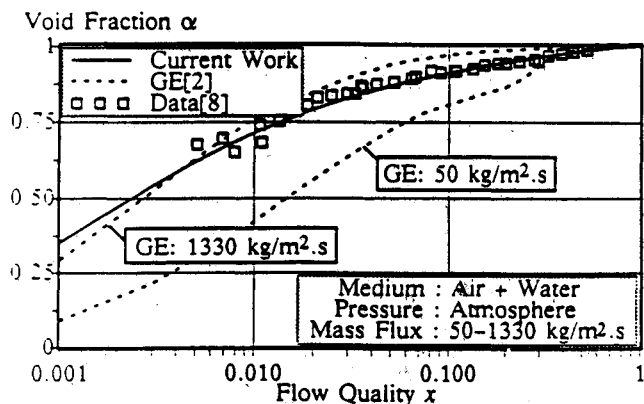


Fig. 7 Current work and correlation compared with air–water data. Data covers the complete mass flux range.

higher void fraction than the current formula in the region of high flow qualities of Fig. 4. This appears indeed to be the case, if one accepts the two correlations to be representative of the data trend. The corresponding slip curves of the correlations are shown in Figs. 5 and 6. At high flow qualities the correlations do not satisfy the endpoint conditions on slip.

A case of low entropy production is the adiabatic air–water data base from Ref. 8, shown in Fig. 7. It contains a 25-fold mass flux variation. The GE correlation is plotted for the two extreme values of mass fluxes in the data. It envelopes the data but the current formula performs more satisfactorily. The EPRI correlation could not be plotted in this comparison because it requires the critical pressure as input. If, however, the critical pressure of water is employed, it performs analogous to the GE correlation.

### Concluding Remarks

The analysis presented takes no account of any irreversibilities due to wall or phase shear, heat flux, or other mechanisms. It is fully idealized and hence should only be valid for a reversible process. However, as indicated earlier, one may expect this formula to closely follow the real behavior for low values of the flow quality and, in particular, the data taken under conditions where the degree of irreversibility is less pronounced. The comparison shown with the air–water data appears to be in line with this hypothesis. The proposed  $\alpha$ – $x$  relation is characterized by explicitness, analytical na-

ture, and simplicity, permitting also hand calculation. In contrast, the state-of-the-art correlations are implicit, iterative, and complex. Because the formula can be readily integrated and differentiated, it may be applicable to analytical treatments of two-phase flow problems.

Further work should involve an investigation of the applicability of the formula in countercurrent flow cases. Also of relevant interest is the quantitative evaluation of the two-phase process irreversibility in a duct. This may account for the integral effect of mass and heat flux, geometry, surface quality, and other thermal hydraulic characteristics, rather than a mass flux effect alone.

### Acknowledgments

The authors wish to express their appreciation to the contributions made by H. Spierling, W. Kraemer, E. Loehr, and W. Uebelhack at SIEMENS, West Germany, B. Burdick, Advanced Nuclear Fuels Corporation, Washington, USA and S. L. Smith, Berkely Nuclear Laboratory, England, and the support from the West Virginia University Energy and Water Research Center.

### References

- <sup>1</sup>Chexal, B., et al., "A Full-Range Drift Flux Correlation for Vertical Flows," EPRI, Sept. 1986.
- <sup>2</sup>Findlay, J. A., et al., "BWR Void Fraction Correlation," GE NEDE-21933, Aug. 1978.
- <sup>3</sup>Ohkawa, K., et al., "The Analysis of CCFL Using Drift Flux Models," *Nuclear Engineering and Design*, Vol. 61, 1980.
- <sup>4</sup>Holmes, J. A., "Description of the Drift Flux Model in the LOCA-Code RELAP-UK," Conf. on Heat and Fluid Flow in Water Reactor Safety, Manchester, Sept. 13–15, 1977.
- <sup>5</sup>Ishii, M., "1-D Drift Flux Model and Constitutive Equations for Relative Motion Between Phases," ANL-77-47, 1977.
- <sup>6</sup>Zuber, N., and Findlay, J. A., "Average Volumetric Concentration in Two-Phase Flow Systems," *Transactions of the ASME, Journal of Heat Transfer*, Vol. 87, 1965, pp. 453–468.
- <sup>7</sup>Rouhani, S. Z., "Void Measurements in the Region of Subcooled and Low-Quality Boiling," Symposium on Two-Phase Flow, University Exeter, 1966.
- <sup>8</sup>Anderson, G. H., et al., "Liquid Entrainment; Measuring Local Mass Flow Density of Liquid Drops and their Velocity," *Chemical Engineering Science*, Vol. 12, 1960, p. 233.
- <sup>9</sup>Butterworth, D., "A Comparison of Some Void-Fraction Relationships for Co-Current Gas-Liquid Flow," *International Journal of Multiphase Flow*, 1975, pp. 845–850.
- <sup>10</sup>Alia, P. et al., 1965, "Liquid Volume Fraction in Adiabatic Two-Phase Vertical Upflow Round Conduit," CISE Rept. R-105.